PAPER

Check for updates

Interactions between aromatic hydrocarbons and functionalized C_{60} fullerenes – insights from experimental data and molecular modelling†

Thorsten Hüffer,[a] Huichao Sun,[a] James D. Kubicki,[b] Thilo Hofmann*[a] and Melanie Kah*[a]

Understanding molecular interactions between organic compounds and carbon-based nanomaterials is crucial to the interpretation of phase transfer processes, both in technical applications and within the environment. There is, however, little information available on the interactions between organic compounds and C_{60} fullerenes, in particular regarding the effects of functionalization. Experimental sorption isotherms and molecular modelling have therefore been used to systematically investigate how these interactions are affected by functionalization of the sorbate (using one, two and four ring aromatics, with –OH or –NH_2 functional groups) and the sorbent (*i.e.*, C_{60} and C_{60}-OH). Functionalization of the sorbent, as well as hydroxyl- and amino-functionalization of the sorbate, had a significant effect on sorption. The enhanced sorption of hydroxyl- and amino-functionalized sorbates by C_{60} may be due to an increased contribution from π–π electron donor–acceptor interactions. Additional hydrogen bond interactions with C_{60}-OH also appear to play an important role. Our results emphasize that the surface chemistry of C_{60} is of critical importance to their interactions with organic compounds. The ageing of C_{60} in technical applications, or in the environment, is therefore likely to significantly affect the molecular interactions, and hence sorption strength, for polar and non-polar organic compounds.

Environmental significance

Knowledge on the sorption behaviour of C_{60} fullerenes is limited, especially after their surface becomes functionalised as a result of environmental transformation processes. We have combined several experimental approaches to generate a comprehensive sorption dataset for C_{60} and C_{60}(OH) interacting with a series of eight probe sorbates. Computational simulations were run to calculate the energy associated with each molecular interaction. The integration of the experimental and modelling approaches allows a systematic evaluation of the roles that aromaticity and functionalisation play in sorption. The new insight into the sorption behaviour of fullerenes is necessary not only to assess the consequences of their release into the environment, but also to evaluate their performance as sorbent materials in technical applications.

Introduction

Engineered carbon-based nanomaterials (CNMs), including fullerenes (C_{60}) and carbon nanotubes (CNTs), have been attracting increasing attention due to their unique physico-chemical properties. Strong interactions between CNMs and organic compounds, such as polycyclic aromatic hydrocarbons[1] and benzene derivatives,[2] have led to the recognition of CNMs as promising sorbent materials with a number of potential applications, such as in sample preparation for analytical chemistry,[3] or the removal of organic contaminants from the environment.[4] Apart from these beneficial uses of CNMs as sorbents, there is concern about the possible environmental impact of the expected future increase in CNM production, and about the transport and eventual fate of CNMs. The fact that C_{60} also occur naturally emphasizes the importance of studying engineered C_{60} nanomaterials as appropriate models for other carbonaceous sorbents, which are critical in the management of organic pollutants. The interpretation and prediction of molecular interactions between organic compounds and C_{60} in particular is of major importance for understanding phase transfer processes in environmental matrices and assessing the potential use of these materials as sorbents.

[a] Department of Environmental Geosciences and Research Network Environmental Science, University of Vienna, Althanstrasse 14, 1090 Vienna, Austria.
E-mail: thilo.hofmann@univie.ac.at, melanie.kah@univie.ac.at;
Tel: +43 1 4277 53320, +43 1 4277 53381
[b] Department of Geological Sciences, University of Texas at El Paso, 500 West University Avenue, El Paso, TX 79968, USA
† Electronic supplementary information (ESI) available. See DOI: 10.1039/c7en00139h

This journal is © The Royal Society of Chemistry 2017

Environ. Sci.: Nano, 2017, 4, 1045–1053 | 1045

To date, the most frequently discussed interactions governing sorption by CNMs are hydrophobic, π–π electron donor–acceptor (EDA), and hydrogen-bond interactions. There is, however, some controversy regarding the effects that functional groups have on such interactions, depending on whether they are on the sorbent or on the sorbate. While a number of studies have stressed the importance of hydrophobic interactions in sorption,[1,5,6] there are other reports of poor correlation between sorption and sorbate hydrophobicity.[7] Strong sorption of hydroxyl- and amino-functionalized benzenes and polycyclic aromatic hydrocarbons (PAHs) by CNTs has been ascribed to π–π and n–π EDA interactions.[8,9] In addition to the influence that sorbate properties have on the relative contributions of different molecular interactions, changes in sorbent surface properties also need to be taken into account. The surfaces of CNMs can be functionalized during their production, purification, dispersion, and use, and/or following their release into an aquatic environment.

We have previously investigated the effect of UV-induced surface oxidation on the sorption behavior of C_{60}.[6] If the aforementioned theory of enhanced sorption being due to enhanced π–π and n–π EDA interactions was also relevant for sorbents with functionalized surfaces, such surface oxidation would be expected to result in an increase in sorption. However, the oxidation of C_{60} surfaces actually led to a significant reduction in both the maximum sorption capacity and the sorption affinity, much likely due to the decrease in the surface hydrophobicity. Our results indicated that, in addition to non-specific van der Waals and EDA interactions, the oxidation of C_{60} surfaces may have possibly resulted in a contribution from hydrogen-bond interactions to the overall sorption. The sorbates used in our previous investigation[6] were not diverse enough and did not allow any further investigations into the contribution of hydrogen-bond interactions to the sorption behavior of surface-oxidized C_{60}. Investigations into the sorption of hydroxyl- and amino-functionalized aromatics by graphene oxide nanoparticles have indicated a likely contribution from hydrogen-bond interactions, in addition to EDA interactions.[10]

Compared to CNTs, there is relatively little information available on the sorption behavior of C_{60}. This may be due to difficulties associated with the commonly used batch sorption test set-ups using centrifugation, filtration, or sedimentation to separate the solid and liquid phases. Assessing the impact that functionalization of the sorbent and/or sorbate has on sorption requires data for different sorbent/sorbate combinations that are difficult to measure.

The objective of this research was to improve our understanding of the effect that functionalization and different functional groups have on sorption. Our investigations combined two experimental approaches, passive sampling and headspace analysis, in order to allow the generation of sorption data for a wide range of sorbent and sorbate combinations. Phase-transfer energies were also calculated, using a molecular simulation approach. The results from these three approaches allowed us to make an integrated comparison of the interactions between C_{60} and organic compounds with significantly different physico-chemical properties. The integration of molecular modelling with experimental sorption data is extremely useful in view of the large number of possible organic compounds, especially with respect to making predictions for sorbent/sorbate systems for which experimental data is difficult to acquire.

Experimental

Materials

Fullerenes (C_{60}, 99.5% purity, Sigma-Aldrich, Steinheim, Germany) and polyhydroxyl fullerenes (C_{60}-OH, BuckyUSA, Houston, TX, USA) were used as-purchased. A polyoxymethylene sheet (POM; thickness = 0.5 mm; density = 1.41 g cm^{-3}) was purchased from Vink Kunststoffen BV (Didam, The Netherlands). The POM sheet was cut into strips that were cold-extracted using hexane (30 min) and methanol (3 × 30 min), and subsequently air-dried.[11]

Benzene (99.0%), phenol (99.0%), aniline (99.5%), naphthalene (99.0%), 1-naphthol (99.0%), 1-naphthylamine (99.0%), and 1-hydroxypyrene (98.0%) were purchased from Sigma-Aldrich (Steinheim, Germany). Pyrene (99.5%) and pyrene-d10 (99.5%, internal standard for quantification) were obtained from Dr. Ehrenstorfer GmbH (Augsburg, Germany). Selected physico-chemical properties of the sorbates used in the experiments are listed in Table 1. Methanol, hexane and acetonitrile of residue analysis grade (Lab Scan, Ireland and Acros Organics, Belgium) were used as solvents.

Sorption experiments

Sorption batch experiments were conducted in three-phase systems at room temperature, using 0.01 M NaCl as background solution. Stock solutions were prepared in methanol and the amount spiked was kept below 0.2 vol% to minimize co-solvent effects.

The sorption of volatile and semi-volatile compounds (benzene, phenol, aniline, naphthalene, naphthol, and naphthylamine) by C_{60} and C_{60}-OH was determined by headspace analysis, as described in Hüffer et al.[14] Briefly, 10–50 mg of the sorbent material was weighed into 20 mL amber screw-top headspace vials and 10 mL of the background solution was added into the vials, which were then spiked with sorbate standard solutions. Samples were horizontally shaken at 150 rpm for 7 days to reach equilibrium (kinetics tests were conducted between 3 and 10 days, data not shown). Upon equilibration, the vials were placed in the tray of the autosampler at least 2 hours prior to analysis to allow gaseous and aqueous phase equilibration. Sorbate concentrations in the vial headspaces were determined using in-tube microextraction (ITEX2). The ITEX2 option for the CombiPal autosampler was obtained from Axel Semrau (Sprockhövel, Germany). Extraction was achieved using up to 20 extraction strokes, with aspirating and dispensing volumes of 1 mL at a flow of 50 μL s^{-1}. Following the extraction, 500 μL of helium

1046 | Environ. Sci.: Nano, 2017, **4**, 1045–1053

This journal is © The Royal Society of Chemistry 2017

Table 1 Selected physico-chemical properties of sorbates

Sorbate	$S_w{}^a$ [mg L^{-1}]	p$K_a{}^b$	log $K_{aw}{}^c$	log $K_{ow}{}^d$	log $K_{hw}{}^e$
Benzene	1790	—	−0.65	2.18	2.14
Phenol	82 800	9.99	−4.67	1.46	−0.90
Aniline	36 000	4.60	−4.03	0.90	−0.10
Naphthalene	31	—	−1.72	3.30	3.44
Naphthol	866	9.34	−5.61	2.85	0.52
Naphthylamine	1700	3.92	−4.72	2.25	1.77
Pyrene	0.135	—	−3.44	4.88	
Hydroxypyrene	2.777		−7.85	4.45	

^{a} S_w: water solubility. ^{b} pK_a: acidic dissociation constant. ^{c} log K_{aw}: air–water partitioning constant, calculated using Henry's constant (K_H) (atm dm^3 mol^{-1}), where $K_{aw} = K_H/(RT)$, R = 0.082 (L atm K^{-1} mol^{-1}) and T: temperature (298.15 K). ^{d} log K_{ow}: octanol–water partitioning constant. All data were obtained from ref. 12. ^{e} log K_{hw}: hexadecane–water partitioning constant, calculated using a thermodynamic cycle with log K_{aw} and the hexadecane–air partitioning constant obtained from the UFZ-LSER database.[13]

was aspirated from the injector as a desorption gas. To avoid cross-contamination, the trap was heated to 300 °C for at least 5 minutes between samples while being flushed with nitrogen. For quantification, an external calibration series was prepared one day prior to the analyses, with 10 standards each containing 10 mL of the background solution. All analyses were conducted using an Agilent 6890N gas chromatograph coupled to an Agilent 5975 mass spectrometer (30 m × 250 μm × 0.25 μm, J&W Scientific; isothermal oven temperatures between 50 and 200 °C; helium carrier gas flow of 1.5 mL min^{-1}).

The isotherms of sorption of naphthol, pyrene and hydroxypyrene by C$_{60}$ were measured using a passive sampling method that has been described previously.[6] Briefly, POM strips each weighing about 100 mg were added to the C$_{60}$ suspensions and the samples were subsequently spiked. The samples were then shaken horizontally in the dark at 150 rpm for 28 days, in order to achieve equilibration between the sorbates, C$_{60}$, and the POM strips. Following equilibration, the POM strips were removed from the vials and wiped with a wet tissue. The sorbate concentrations in the POM strips were then analyzed. For those samples initially spiked with pyrene, an internal standard (pyrene-d10) was added and the POM strips were extracted using hexane by accelerated solvent extraction (ASE 200, Dionex USA; 1000 psi, 100 °C). Extracts were concentrated under nitrogen and analyzed using the GC-MS system described above, equipped with an HP-5MS fused silica column (60 m × 250 μm × 0.25 μm, J&W Scientific), in pulsed splitless mode, and at an oven temperature of 55 °C for 1 minute, which was then increased at a rate of 10 °C min^{-1} up to 300 °C. When hydroxypyrene and naphthylamine were used as sorbates, the POM strips were extracted using ASE and acetonitrile as solvent. Following concentration, the samples were analyzed using HPLC (Agilent 1100 high-performance liquid chromatography, USA) with a reversed phase column (Zorbax Eclipse XDB-C18, 4.6 × 150 mm, with a 4.6 × 125 mm PSS polymer-filled guard column, Agilent, USA) and UV detection at 254 nm. The mobile phases for measuring hydroxypyrene and naphthylamine were 20/80 (v/v) acetonitrile/Milli-Q water and 40/60 (v/v) acetonitrile/acetate buffer (pH = 4.7), respectively. Selected qual-

ity parameters of the ASE-HPLC method are shown in Table S1 in the ESI.†

The sorption isotherms were fit with the Freundlich model using Sigma Plot 12.0 for Windows:

$$C_s = K_F C_w{}^n \qquad (1)$$

where C_s [μg kg^{-1}] and C_w [μg L^{-1}] denote the sorbed and aqueous concentrations of sorbates, respectively, and K_F [(μg kg^{-1}) per (μg L^{-1})$^{1/n}$] and n [—] are the Freundlich affinity coefficient and linearity exponent, respectively.

Computational modelling

The models were created using Materials Studio 7 (MS 7) software (Accelrys Inc., San Diego, CA). Models were drawn in the visualizer module and then subjected to the "Clean" tool to generate the starting structures, except for the C$_{60}$ and C$_{60}$-OH models. The C$_{60}$ model was taken directly from the MS 7 library and the C$_{60}$-OH model was created by adding 24 hydroxyl groups to the C$_{60}$ model, guided by the structure used by Maciel *et al.*[15] In order to form the dimer models, the aromatic compounds and their functionalized derivatives were placed approximately 3.5 Å from the surface of the C$_{60}$ or C$_{60}$-OH models, which represents the favored distance for aromatic–aromatic interactions.[16]

Both individual and dimer models were then subjected to energy minimization in the Gaussian 09 (ref. 17) program using the M05-2X exchange correlation functional[18] and the 6-311+G(d,p) basis set.[19] Configurations after energy minimization are shown in Fig. S1 in the ESI.† M05-2X was selected because it includes dispersion corrections that are capable of reproducing aromatic–aromatic interactions[20] to compensate for the lack of dispersion in density functional theory (DFT) calculations. The 6-311+G(d,p) basis set was chosen because it was the largest basis set that could be used within the practical computational limits available. This triply split (6-311) basis set allows improved representation of aromaticity, the diffuse function on heavy elements (*i.e.*, non-hydrogen atoms) helps to account for electron distribution between monomers, and the polarization functions are necessary to

describe aromatic molecules and their interactions (Foresman and Frisch, 2015 and references therein).[21] The self-consistent electron density convergence was set to a non-default value of 10^{-6} Hartrees in order to allow more efficient calculations. The integral equation formula polarized continuum model was used to take into account water solvation effects. All atoms were allowed to relax with no symmetry constraints and energies were minimized to 10^{-6} Hartrees per molecule (1 kJ mol^{-1}). Energy difference (ΔE) values were calculated as the energy differences between the dimer and the two monomers (*e.g.*, $\Delta E = E(C_{60} + \text{benzene}) - E(C_{60}) - E(\text{benzene})$). The ΔE values should be similar to the ΔH of dimerization because the PV term is small at atmospheric pressures.

Results and discussion

Sorption of non-functionalized aromatics by C_{60}

The sorption isotherms of non-functionalized aromatic hydrocarbons followed the order of benzene < naphthalene < pyrene (Fig. S2†), in accordance with previous reports on the sorption of aromatic sorbates by C_{60} and CNTs.[5,6] The number of π electrons in the sorbate increases as the number of aromatic rings increases, which suggests that enhanced π–π EDA interactions are of major importance within these systems. An increase of approximately 12–13 kJ mol^{-1} for every additional aromatic ring was calculated by computational modelling (ΔE values calculated for dimer formation in water are listed in Table S2†), which is similar to the figure previously calculated by Zou *et al.*[22] for CNTs (9–10 kJ mol^{-1}). Comparing the sorption energies that we calculated in this study for C_{60} with those obtained by Zou *et al.*[22] yields the following relationship (Fig. S3†):

$$\Delta E_{C_{60}} = 1.36\Delta E_{CNT} + 34.54 \quad (n = 6, R^2 = 0.9885, p < 0.01) \quad (2)$$

Sorption by C_{60} and CNTs is expected to be driven by van der Waals and EDA interactions between delocalized π-electron systems of the sorbent and the sorbate, as it is for soot.[23] Eqn (2) indicates that sorption by CNTs is stronger than sorption by C_{60}, which is also suggested when comparing our experimental data with data obtained for CNTs.[5,14] Stronger sorption by CNTs than by C_{60} is attributed to their larger surface area, micropore and mesopore volumes.[1] Further, the C_{60} cage-like structure consists of twelve 5-carbon rings, which may reduce the extent of charge delocalization compared to CNTs and results in a chemical behavior between an aromatic and aliphatic conjugated carbon chain.[4] Kubicki previously calculated the energies associated with the interaction between 13 aromatic hydrocarbons and a coronene molecule (as a model for soot).[23] Sorption energies calculated for coronene were greater (−86, −128, and −173 kJ mol^{-1} for benzene, naphthalene, and pyrene, respectively) than those for sorption by C_{60} (Table S2†). The discrepancy between the calculated data for C_{60} and coronene as a model soot surface may have to be investigated in the future because C_{60} is often used as a model for carbonaceous sorbents such as soot.

Effect of sorbate functionalization on sorption

Our experimental data for the sorption of benzene and naphthalene, together with their functionalized analogues, by C_{60} provided reasonable fits for all isotherms with the Freundlich model ($R^2 > 0.92$, Fig. 1). The linearity of the isotherms varied between different sorbate–sorbent systems, with *n*-values ranging from 0.569 for phenol to 0.961 for naphthylamine. There was no correlation between the *n*-values and the sorbate properties (*i.e.*, hydrophobicity or molecular volume), which is in agreement with recent reports on sorption by CNTs.[24]

The isotherm data shown in Fig. 1a indicate weaker sorption of benzene and phenol than that of aniline. For the naphthalene series (Fig. 1b), sorption increased in the order naphthalene < naphthol < naphthylamine. Not all sorption isotherms overlapped, due to the broad range of sorbate properties. In order to compare sorption data, distribution coefficients were calculated at 10^{-4} of each sorbate's aqueous solubility, using the Freundlich parameters (Table 2). This concentration was chosen because experimental isotherm data were available for most of the sorbates at this concentration, thus minimizing the need for extrapolations. The calculated distribution coefficients showed no consistent correlation with the sorbate hydrophobicity (Fig. S4†). In fact, the sorption of hydroxyl- and amino-functionalized sorbates was stronger than the sorption of non-functionalized compounds (Table 2). If sorption by C_{60} was dominated by hydrophobic interactions, then the sorption of non-functionalized sorbates should have been much stronger than the sorption of functionalized compounds. Significant correlations between distribution coefficients and sorbate hydrophobicity have previously been observed for PAHs and CNMs,[5,6] but no correlation was obtained for sorbates with different functional groups.[7,10,25] This is to be expected because correlations with the octanol–water partition constant (K_{ow}) that are compound-class specific cannot be directly extrapolated to class-comprehensive interactions.[26]

Two additional processes have previously been discussed in relation to the sorption of hydroxyl-functionalized sorbates by CNM sorbents: loss of sorbates by transformation[27] and oxygen-induced oxidative coupling.[28] Both mechanisms could result in an overestimation of the contribution of π–π EDA interactions to sorption by C_{60}. Blank vials containing the spiked background solution with no sorbent showed that any loss of sorbates resulting from light-induced transformation processes was minimal (<5%), and in fact no losses should have occurred as all vials were covered with aluminum foil. Oxygen-induced oxidative coupling of hydroxyl-functionalized sorbates has been shown to affect their sorption by carbonaceous sorbents, but the precise mechanisms controlling the reaction are not yet fully understood.[29–33] The reaction takes place preferentially on the sorbent surfaces rather than
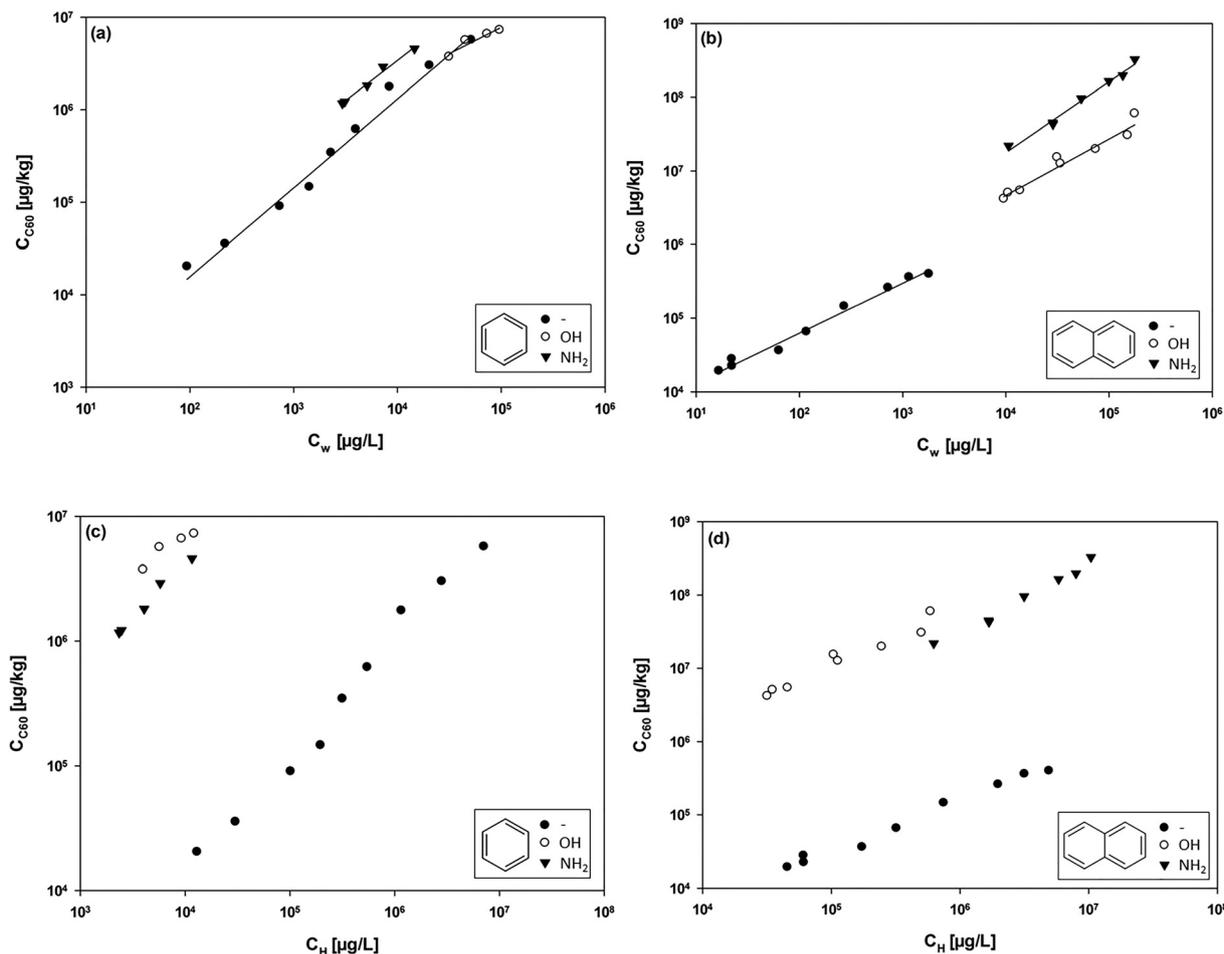
Fig. 1 Experimental sorption data for C_{60}: original data for (a) benzene and (b) naphthalene derivatives, and sorption data normalized for hydrophobicity with hexadecane as a reference solvent for (c) benzene and (d) naphthalene derivatives. Solid lines indicate Freundlich model fits.

within the solution, with the dissociation of the sorbate's hydroxyl functional groups resulting in enhanced oxidative coupling; the presence of acidic surface functional groups on the sorbent may reduce the strength of the coupling.[28] The contribution of oxidative coupling in our investigations can be assumed to be minimal because (1) the suspension pH values (ranging between 6.3 and 6.8) were below the pK_a values of the hydroxyl-functionalized sorbates (9.99 and 9.34 for phenol and naphthol, respectively), (2) the contribution of this reaction between naphthol and multi-walled CNTs has recently been shown to be minimal,[34] and (3) the increase in

sorption of hydroxyl-functionalized sorbates was greater than that typically observed for oxidative coupling.[29–33,35]

The stronger sorption in the presence of hydroxyl and amino functional groups on the sorbates therefore suggests the occurrence of additional interactions in response to hydrophobic effects, such as EDA or hydrogen-bond interactions. In order to investigate the possible contribution of non-hydrophobic interactions to the overall sorption, sorption isotherm data were normalized by dividing the sorbate aqueous concentrations (C_w) by the hexadecane–water partition constant, K_{hw} (values are shown in Table 1).[7,24]

The K_{hw}-normalized isotherms of the benzene and the naphthalene series are shown in Fig. 1c and d, respectively. At a given normalized concentration, the sorbed concentrations of hydroxyl- and amino-functionalized sorbates were almost two orders of magnitude higher than those of non-functionalized benzene and naphthalene. The enhanced non-hydrophobic interactions for the functionalized sorbates can be explained by additional hydrogen-bond and/or EDA interactions. The occurrence of hydrogen bonding is supported by the stronger sorption of the hydroxyl-functionalized sorbates than that of the amino-functionalized sorbates

Table 2 Results of the Freundlich model fit of C_{60} isotherm data, regression coefficients, and calculated distribution coefficients

Sorbate	K_F [(μg kg^{-1}) per (μg L^{-1})$^{1/n}$]	n [—]	R^2	$\log K_d$, 10^{-4}
Benzene	118.4	0.960	0.970	1.98
Phenol	11 050.5	0.569	0.922	2.35
Aniline	1112.3	0.872	0.987	2.59
Naphthalene	2742.2	0.679	0.980	3.22
Naphthol	5840.5	0.768	0.944	3.27
Naphthylamine	28 440.6	0.961	0.971	3.33

This journal is © The Royal Society of Chemistry 2017

Environ. Sci.: Nano, 2017, **4**, 1045–1053 | **1049**

(Fig. 1c and d). Oxygen is more electronegative than nitrogen and the hydroxyl group is therefore more likely to engage in hydrogen bonds than the amino group. Enhanced non-hydrophobic interactions for the functionalized sorbates can also be explained in terms of enhanced π–π EDA interactions, because the electron-donating capability of the aromatic benzene ring is enhanced by the presence of hydroxyl and amino functional groups. Both functional groups are electron donors and allow the sorbate to interact more strongly with the electron-depleted regions of C_{60} (π-electron acceptor) than the non-functionalized sorbates.[36] The stronger sorption of the amino-functionalized sorbates (Hammett constant of -0.66)[37] relative to the hydroxyl-functionalized sorbates (Hammett constant of -0.37)[37] is also consistent with the conclusion that enhanced π–π EDA interactions are of major importance for sorption by C_{60}.

Modelling indicates that for the C_{60}, interactions were more thermodynamically favorable in the order non-functionalized sorbate < hydroxyl-functionalized sorbate < amino-functionalized sorbate. In order to compare the experimental results with the modelling data, the experimental free energy change of phase transfer (ΔG_{exp}, Table S2†) was calculated using:

$$\Delta G_{exp} = -RT \ln K_d \tag{3}$$

where R denotes the universal gas constant (8.314 J mol^{-1} K^{-1}), T represents the temperature at which the experiments were conducted (298.15 K), and K_d is the distribution coefficient derived from our experiments. The calculated energies correlated significantly ($p < 0.01$) with the experimental free energy changes (Fig. 2) but clearly deviated from a 1:1 line (we note that the main difference between the ΔE and ΔG is the $T\Delta S$ term. A linear relationship suggests that $T\Delta S$ is reasonably constant in this case). A 2.3-fold overestimation of
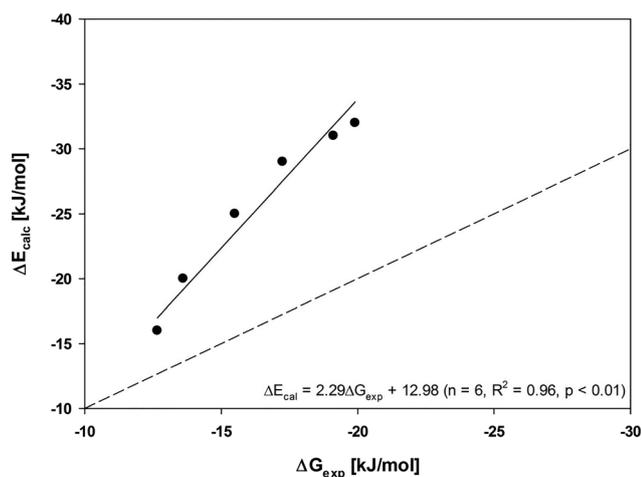
the data from model calculations compared to the experimental data can be ascribed to the fact that the calculations considered C_{60} sorbents with an ideal and homogeneous outer surface. Heterogeneous surface properties (*i.e.*, groove, interstitial, and pore sorption sites), probably resulting from the formation of aggregates, may have an impact on the experimental data. The modelled data only takes into account surface sorption and ignores any interactions within the pores of the sorbent aggregates.[23] Future work could consider aggregated sorbents and absorption into pores to test whether these factors are the main sources of the discrepancies. This issue is critical because diffusion out of such micropores may present a kinetic barrier, in addition to the thermodynamic barrier of adsorption ΔG.[38]

Effect of sorbent functionalization on sorption

An increase in sorption by graphene oxide nanoparticles (GONPs) has been previously reported to occur when the sorbates are functionalized.[10] Sorption by GONPs was also clearly more linear than sorption by CNTs (whether oxidized or not), which was attributed to differences in the morphologies of the aggregates. The distribution coefficients for GONPs increased by approximately one order of magnitude when re-calculated for the concentration ranges used in this study. Both GONPs and C_{60}-OH are highly dispersed compared to CNTs (which tend to remain as large aggregates, or form bundles), with more surface area available for sorption.[6] The high levels of dispersion result in a more homogeneous distribution of sorption site energies and thus in greater sorption linearity.[25,39,40] Our experimental sorption data and computational modelling indicated an increase in sorption by C_{60}-OH, from the non-functionalized sorbates to amino-functionalized sorbates, and even greater sorption for hydroxyl functionalization (Tables 3 and S2†).

Sorbate functionalization results in a number of different interactions that may have contributed to the sorption by C_{60}-OH (*i.e.*, hydrogen–π, Lewis acid–base, and hydrogen-bond interactions). Hydrogen–π interactions between the electron-rich benzene moieties of the sorbates and hydrogen on the functionalized surface cannot sufficiently explain the large increase in sorption observed. The NH–π interactions occur with energies between 6 and 7 kJ mol^{-1} (ref. 36) but the increased interaction energies obtained from both

Fig. 2 Regression between the experimental ΔG_{exp} and ΔE_{calc} values obtained from the calculations for sorption by C_{60}. The dashed line indicates the 1:1 line.

$\Delta E_{cal} = 2.29\Delta G_{exp} + 12.98$ (n = 6, R^2 = 0.96, p < 0.01)

Table 3 Sorption coefficients (log K_d) for benzene and naphthalene sorbates sorbed by C_{60}-OH at given concentrations relative to the sorbate solubilities

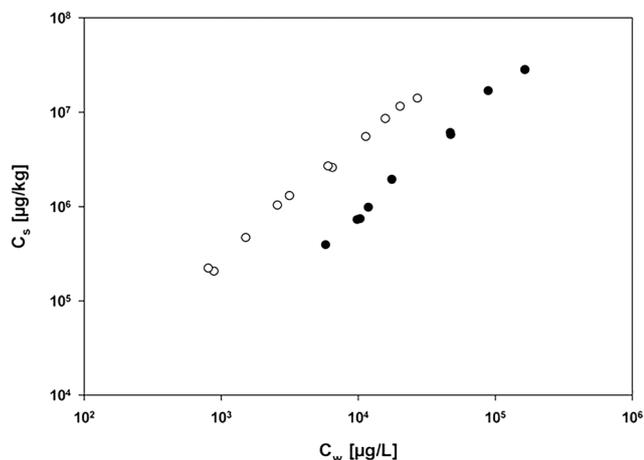| Sorbate	log K_d	C_w/S_w [—]
Benzene	1.89 ± 0.09	$10^{-4.3}$
Phenol	2.95 ± 0.06	$10^{-4.2}$
Aniline	2.52 ± 0.14	$10^{-4.4}$
Naphthalene	2.37 ± 0.10	$10^{-2.0}$
Naphthol	4.32 ± 0.13	$10^{-2.2}$
Naphthylamine	3.93 ± 0.11	$10^{-1.9}$

± standard deviation ($n = 3$).

Fig. 3 Isotherms for sorption of naphthylamine by C_{60} using ($\circ$) POM passive sampling and ($\bullet$) headspace analysis approaches.

methodological approaches were clearly larger. Lewis acid–base interactions between the amino-functionalized sorbates (base) and C_{60}-OH (acid) could also have contributed to sorption,[7] as has previously been suggested to explain the enhanced sorption of aniline and pyrimidine by functionalized CNTs.[41] However, Lewis acid–base interactions alone cannot explain the strong sorption of functionalized sorbates by C_{60}-OH, as the sorption enhancement was not restricted to amino-functionalized sorbates. The fact that sorption was the strongest for hydroxyl-functionalized sorbates rather points to a major contribution from hydrogen-bond interactions. This is supported by the fact that for non-functionalized sorbates, sorption by C_{60}-OH was lower than sorption by C_{60} (-Tables 2, 3 and S2†). Hydrogen-bond interactions (as well as others) have previously been suggested to contribute significantly to the sorption of amino- and hydroxyl-functionalized sorbates by GONPs,[10] although this is difficult to demonstrate experimentally. The large increases in the sorption of hydroxyl-functionalized sorbates by C_{60} and C_{60}-OH in our experiments, which are also reflected in similar results obtained from computational modelling (Table S2†), suggest that hydrogen-bond interactions are likely to have played a very important role in the sorption by C_{60}-OH.

It is noteworthy that the sorption of non-functionalized sorbates to C_{60}-OH was lower than that to C_{60}. This is in accordance with a previous study in which use of the polyoxymethylene (POM) passive sampling method has led to the (partial) oxidation of C_{60}, which was confirmed by XPS and FT-IR data, and reduced sorption of non-functionalized hydrophobic organic compounds.[6] However, the range of PAHs used as probe sorbates was not sufficiently diverse to allow further investigations into the effect that changes in surface properties have on molecular interactions contributing to the overall sorption. To this end, sorption isotherms obtained using the POM passive sampling and headspace analysis approaches were directly compared, using naphthylamine as a probe compound for which experimental data could be determined using both methods. Sorption was stronger when mea-

sured using the POM passive sampling method than when using headspace analysis (Fig. 3). This clearly supports previous observations that using the POM passive sampling method results in a method-induced modification of the C_{60} sorbent particles. The potential effects of the long equilibration time for the POM passive sampling method are (i) the mechanical breakdown of large C_{60} aggregates (possibly resulting in an increase in maximum sorption capacity) and (ii) oxidation of C_{60} surfaces (thus reducing their hydrophobicity and interactions with non-polar sorbates[6]). This conclusion is supported by ΔE values of -32 and -55 kJ mol^{-1} calculated for C_{60}–naphthylamine and C_{60}-OH–naphthylamine interactions, respectively. A reduction in sorbent hydrophobicity would reduce the contribution from hydrophobic non-polar interactions. The results obtained for naphthylamine suggest that oxidation of the C_{60} surfaces allowed additional hydrogen-bond interactions to occur between functionalized sorbates and oxygen-containing functional groups on the C_{60} surfaces, which would explain the large increase in the sorption of naphthylamine by surface-modified C_{60}.[10] A contribution from additional hydrogen bond interactions was also indicated by isotherms for the sorption of pyrene and hydroxypyrene by C_{60} using the POM passive sampling method (Fig. S5†), which showed that sorption of hydroxypyrene by oxidized C_{60} was stronger than that of pyrene. A reduction in ΔE values from pyrene to hydroxypyrene was only obtained for C_{60}-OH (Table S2†), while relatively unchanged ΔE values were obtained for the interactions between pyrene and C_{60}, and between hydroxypyrene and C_{60}. The results of the experimental comparison and the computational modelling have clear implications for those molecular interactions between organic compounds and CNMs that are susceptible to ageing-induced surface modification following their release into the environment.

Conclusions

This study has, for the first time, evaluated the effects of functionalization of C_{60} sorbents and aromatic hydrocarbon sorbates, by combining experimental data and computational modelling. The results clearly indicate that the relative importance of different molecular interactions is dependent on which functional groups are present, and that functionalization on the sorbent, or on the sorbates, can either enhance or reduce sorption. Differences between sorption by the C_{60} and C_{60}-OH used as model sorbents indicate possible ageing-induced changes in relevant molecular interactions between the nanoparticles and organic compounds, in both technical applications and the environment.

Acknowledgements

This journal is © The Royal Society of Chemistry 2017

Environ. Sci.: Nano, 2017, **4**, 1045–1053 | **1051**

References

1 K. Yang, L. Z. Zhu and B. S. Xing, Adsorption of polycyclic aromatic hydrocarbons by carbon nanomaterials, *Environ. Sci. Technol.*, 2006, **40**(6), 1855–1861.

2 X. L. Wang, J. L. Lu and B. S. Xing, Sorption of organic contaminants by carbon nanotubes: Influence of adsorbed organic matter, *Environ. Sci. Technol.*, 2008, **42**(9), 3207–3212.

3 T. Hüffer, X. L. Osorio, M. A. Jochmann, B. Schilling and T. C. Schmidt, Multi-walled carbon nanotubes as sorptive material for solventless in-tube microextraction (ITEX2)-a factorial design study, *Anal. Bioanal. Chem.*, 2013, **405**(26), 8387–8395.

4 M. S. Mauter and M. Elimelech, Environmental applications of carbon-based nanomaterials, *Environ. Sci. Technol.*, 2008, **42**(16), 5843–5859.

5 M. Kah, X. Zhang, M. T. O. Jonker and T. Hofmann, Measuring and Modelling Adsorption of PAHs to Carbon Nanotubes Over a Six Order of Magnitude Wide Concentration Range, *Environ. Sci. Technol.*, 2011, **45**(14), 6011–6017.

6 T. Hüffer, M. Kah, T. Hofmann and T. C. Schmidt, How Redox Conditions and Irradiation Affect Sorption of PAHs by Dispersed Fullerenes (nC60), *Environ. Sci. Technol.*, 2013, **47**(13), 6935–6942.

7 W. Chen, L. Duan, L. L. Wang and D. Q. Zhu, Adsorption of hydroxyl- and amino-substituted aromatics to carbon manotubes, *Environ. Sci. Technol.*, 2008, **42**(18), 6862–6868.

8 O. G. Apul and T. Karanfil, Adsorption of synthetic organic contaminants by carbon nanotubes: A critical review, *Water Res.*, 2015, **68**, 34–55.

9 L. Hou, D. Q. Zhu, X. M. Wang, L. L. Wang, C. D. Zhang and W. Chen, Adsorption of phenanthrene, 2-naphthol, and 1-naphthylamine to colloidal oxidized multiwalled carbon nanotubes: Effects of humic acid and surfactant modification, *Environ. Toxicol. Chem.*, 2013, **32**(3), 493–500.

10 F. Wang, J. J. H. Haftka, T. L. Sinnige, J. L. M. Hermens and W. Chen, Adsorption of polar, nonpolar, and substituted aromatics to colloidal graphene oxide nanoparticles, *Environ. Pollut.*, 2014, **186**, 226–233.

11 M. T. O. Jonker and A. A. Koelmans, Polyoxymethylene solid phase extraction as a partitioning method for hydrophobic organic chemicals in sediment and soot, *Environ. Sci. Technol.*, 2001, **35**(18), 3742–3748.

12 S. R. Corporation, Interactive PhysProp Database Demo, http://www.syrres.com/esc/physdemo.htm (01.02.).

13 S. Endo, N. Watanabe, N. Ulrich, G. Bronner and K.-U. Goss, *UFZ-LSER database v 2.1 In Research-UFZ*, ed. H. C. f. E., 2015.

14 T. Hüffer, S. Endo, F. Metzelder, S. Schroth and T. C. Schmidt, Prediction of sorption of aromatic and aliphatic organic compounds by carbon nanotubes using poly-parameter linear free-energy relationships, *Water Res.*, 2014, **59**, 295–303.

15 C. Maciel, E. E. Fileti and R. Rivelino, Assessing the solvation mechanism of C-60(OH)(24) in aqueous solution, *Chem. Phys. Lett.*, 2011, **507**(4–6), 244–247.

16 J. D. Kubicki and S. E. Apitz, Models of natural organic matter and interactions with organic contaminants, *Org. Geochem.*, 1999, **30**(8B), 911–927.

17 M. J. Frisch, G. W. Trucks, H. B. Schlegel, G. E. Scuseria, M. A. Robb, J. R. Cheeseman, G. Scalmani, V. Barone, B. Mennucci, G. A. Petersson, H. Nakatsuji, M. Caricato, X. Li, H. P. Hratchian, A. F. Izmaylov, J. Bloino, G. Zheng, J. L. Sonnenberg, M. Hada, M. Ehara, K. Toyota, R. Fukuda, J. Hasegawa, M. Ishida, T. Nakajima, Y. Honda, O. Kitao, H. Nakai, T. Vreven, J. A. Montgomery Jr., J. E. Peralta, F. Ogliaro, M. J. Bearpark, J. Heyd, E. N. Brothers, K. N. Kudin, V. N. Staroverov, R. Kobayashi, J. Normand, K. Raghavachari, A. P. Rendell, J. C. Burant, S. S. Iyengar, J. Tomasi, M. Cossi, N. Rega, N. J. Millam, M. Klene, J. E. Knox, J. B. Cross, V. Bakken, C. Adamo, J. Jaramillo, R. Gomperts, R. E. Stratmann, O. Yazyev, A. J. Austin, R. Cammi, C. Pomelli, J. W. Ochterski, R. L. Martin, K. Morokuma, V. G. Zakrzewski, G. A. Voth, P. Salvador, J. J. Dannenberg, S. Dapprich, A. D. Daniels, Ö. Farkas, J. B. Foresman, J. V. Ortiz, J. Cioslowski and D. J. Fox, *Gaussian 09*, Gaussian, Inc., Wallingford, CT, USA, 2009.

18 Y. Zhao, N. E. Schultz and D. G. Truhlar, Design of density functionals by combining the method of constraint satisfaction with parametrization for thermochemistry, thermochemical kinetics, and noncovalent interactions, *J. Chem. Theory Comput.*, 2006, **2**(2), 364–382.

19 A. D. McLean and G. S. Chandler, Contracted Gaussian-basis sets for molecular calculations .1. 2ND row atoms, Z=11-18, *J. Chem. Phys.*, 1980, **72**(10), 5639–5648.

20 Y. Zhao and D. G. Truhlar, Density functionals for noncovalent interaction energies of biological importance, *J. Chem. Theory Comput.*, 2007, **3**(1), 289–300.

21 J. B. Foresman and A. Frisch, *Exploring Chemistry with Electronic Structure Methods*, 3rd edn, Gaussian Inc., 2015.

22 M. Y. Zou, J. D. Zhang, J. W. Chen and X. H. Li, Simulating Adsorption of Organic Pollutants on Finite (8,0) Single-Walled Carbon Nanotubes in Water, *Environ. Sci. Technol.*, 2012, **46**(16), 8887–8894.

23 J. D. Kubicki, Molecular simulations of benzene and PAH interactions with soot, *Environ. Sci. Technol.*, 2006, **40**(7), 2298–2303.

24 W. Chen, L. Duan and D. Q. Zhu, Adsorption of polar and nonpolar organic chemicals to carbon nanotubes, *Environ. Sci. Technol.*, 2007, **41**(24), 8295–8300.

25 B. Pan and B. S. Xing, Adsorption Mechanisms of Organic Chemicals on Carbon Nanotubes, *Environ. Sci. Technol.*, 2008, **42**(24), 9005–9013.

26 S. Endo, P. Grathwohl, S. B. Haderlein and T. C. Schmidt, LFERs for Soil Organic Carbon-Water Distribution Coefficients (K-OC) at Environmentally Relevant Sorbate Concentrations, *Environ. Sci. Technol.*, 2009, **43**(9), 3094–3100.

27 A. Bhandari, F. X. Xu, D. E. Koch and R. P. Hunter, Peroxidase-Mediated Polymerization of 1-Naphthol: Impact

1052 | *Environ. Sci.: Nano*, 2017, **4**, 1045–1053

This journal is © The Royal Society of Chemistry 2017

of Solution pH and Ionic Strength, *J. Environ. Qual.*, 2009, **38**(5), 2034–2040.

28 J. Jiang, S. Y. Pang and J. Ma, Comment on "Adsorption of Hydroxyl- and Amino-Substituted Aromatics to Carbon Nanotubes", *Environ. Sci. Technol.*, 2009, **43**(9), 3398–3399.

29 R. D. Vidic and M. T. Suidan, Role of dissolved-oxygen on the adsorptive capacity of activated carbon for synthetic and natural organic-matter, *Environ. Sci. Technol.*, 1991, **25**(9), 1612–1618.

30 R. D. Vidic, M. T. Suidan and R. C. Brenner, Oxidative coupling of phenols on activated carbon - impact on adsorption equilibrium, *Environ. Sci. Technol.*, 1993, **27**(10), 2079–2085.

31 Q. L. Lu and G. A. Sorial, Adsorption of phenolics on activated carbon - impact of pore size and molecular oxygen, *Chemosphere*, 2004, **55**(5), 671–679.

32 A. C. D. Pimenta and J. E. Kilduff, Oxidative coupling and the irreversible adsorption of phenol by graphite, *J. Colloid Interface Sci.*, 2006, **293**(2), 278–289.

33 C. H. Tessmer, R. D. Vidic and L. J. Uranowski, Impact of oxygen-containing surface functional groups on activated carbon adsorption of phenols, *Environ. Sci. Technol.*, 1997, **31**(7), 1872–1878.

34 W. H. Wu, W. Jiang, W. X. Xia, K. Yang and B. S. Xing, Influence of pH and surface oxygen-containing groups on multiwalled carbon nanotubes on the transformation and adsorption of 1-naphthol, *J. Colloid Interface Sci.*, 2012, **374**, 226–231.

35 W. Chen, L. Duan, L. L. Wang and D. Q. Zhu, Response to Comment on "Adsorption of Hydroxyl- and Amino-Substituted Aromatics to Carbon Nanotubes", *Environ. Sci. Technol.*, 2009, **43**(9), 3400–3401.

36 M. Keiluweit and M. Kleber, Molecular-Level Interactions in Soils and Sediments: The Role of Aromatic pi-Systems, *Environ. Sci. Technol.*, 2009, **43**(10), 3421–3429.

37 C. Hansch, A. Leo and R. W. Taft, A survey of hammett substituent constants and resonance and field parameters, *Chem. Rev.*, 1991, **91**(2), 165–195.

38 J. J. Pignatello, Bioavailability of Contaminants in Soil, in *Advances in Applied Bioremediation*, ed. A. Singh, R. C. Kuhad and O. P. Ward, Springer-Verlag Berlin, Berlin, 2009, vol. 17, pp. 35–71.

39 J. Y. Chen, W. Chen and D. Zhu, Adsorption of nonionic aromatic compounds to single-walled carbon nanotubes: Effects of aqueous solution chemistry, *Environ. Sci. Technol.*, 2008, **42**(19), 7225–7230.

40 M. Kah, X. R. Zhang and T. Hofmann, Sorption behavior of carbon nanotubes: Changes induced by functionalization, sonication and natural organic matter, *Sci. Total Environ.*, 2014, **497**, 133–138.

41 L. L. Wang, D. Q. Zhu, L. Duan and W. Chen, Adsorption of single-ringed N- and S-heterocyclic aromatics on carbon nanotubes, *Carbon*, 2010, **48**(13), 3906–3915.

This journal is © The Royal Society of Chemistry 2017

Environ. Sci.: Nano, 2017, **4**, 1045–1053 | 1053